

Interwell report

Seismic inversion and reservoir characterization

Léna Pitek and Merli Endamne Obiang

December 2022

Table of contents

1	Introduction	2
2	Importing data	2
2.1	QC seismic data.....	2
2.2	QC data across horizons.....	4
2.3	QC well data.....	6
3	Wavelet shape estimation	7
3.1	Preliminary estimation of the elastic wavelet by MCA	8
3.2	Wavelet optimisation from well data	9
3.3	Final wavelet	12
4	Reverse	13
4.1	Building the initial model.....	13
4.2	Model-based inversion	13
5	Inversion results	14
5.1	Synthetic Seismic	14
5.2	Comparison of synthetic and real seismic data	15
5.3	QC on inversion by comparison with real data	15
6	Conclusion	16

1 Introduction

Seismic inversion is the process of inverting seismic trace data to obtain a subsurface reflectivity log and then an impedance log. Seismic inversion requires extensive pre-processing of the data. These include all the filtering methods used to attenuate noise and thus increase the SNR (Signal to Noise Ratio), methods for sorting seismic traces into common medium points (CMP) in the case of seismic reflection, static and dynamic correction methods of the normal move-out (NMO) type, construction of a velocity model and time or depth migration methods.

The classic seismic inversion that we are going to present is based on a workflow carried out using the Interwell inversion software from Beicip-franlab, a subsidiary of IFPEN. The seismic inversion tools provided by the InterWell software enable several types of reservoir to be modelled. This is a key step in seismic workflows for reservoir E&P (Exploration and Production). It improves data quality by providing fundamental knowledge of reservoir properties and fault networks. This modelling makes it possible to obtain prediction models (risk, pore pressure, lithology, etc.). The aim of inversion is to estimate impedances from seismic data. These impedances will then be used to obtain estimates of poro-elastic parameters, for example. The first step in this work is to link the seismic data, the geological data and the well data. Next, we will estimate the wavelet shape and build the a priori impedance model. Finally, the last part will deal with the inversion and the synthetic seismic obtained.

2 Importing data

The first step in processing is, of course, to load the data into the software: the seismic data, the horizons and the wells. To do this, we need to define the geometry of our dataset, but Interwell can also identify the geometry automatically. In addition, there is a specification for the type of data stacked. Interwell can handle different types of stack: Full-Stack for an angle of incidence of 0° , Near-stack for low angles of incidence, Mid-stack for medium angles of incidence and Far-stack for high angles of incidence. These different stacks are obtained from different sortings on the common medium points (CMP). In this study, we mainly processed full-stack data. Near/Mid/Far-stack data enabled us to make comparisons with our fullstack dataset.

2.1 QC seismic data

In this section, we carried out a quality control of our seismic cube. This is an important step, as it enables us to check the quality of the data and ensure that our seismic is suitably conditioned for inversion. The spectrum is filtered to retain the frequencies essential for inversion, but also to check the quality of the amplitudes. Figure 1 shows a view of inline 100 of our seismic cube.

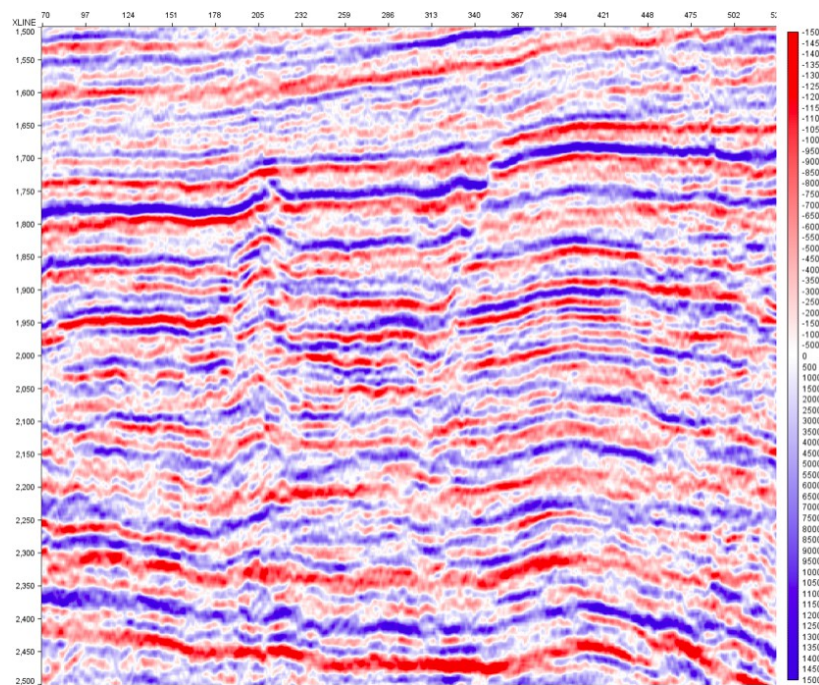


FIGURE 1 - Full Stack seismic section at inline 100: Positive amplitudes in red, negative in blue

We calculated the spectrum of this seismic section in order to determine its frequency content. The spectrum was calculated over the entire seismic section, and we were able to isolate three modes visible in Figure 2. There is a high-amplitude mode at around 25 Hz, and two other secondary modes at 125 Hz and 200 Hz. The mode at 25 Hz is fairly consistent with the usual band of seismic data, and representative of good data.

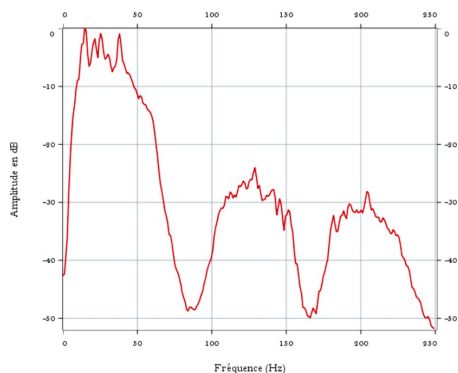


FIGURE 2 - Spectrum of the seismic section at inline 100

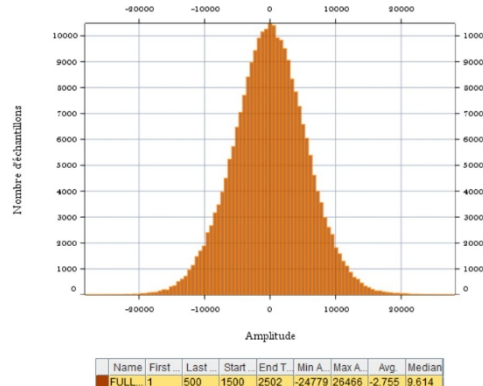


FIGURE 3 - Histogram corresponding to the seismic section at inline 100

Another way of looking at the frequency content is to analyse the spectrogram of our seismic section. Figure 5 shows two spectrograms taken respectively from the entire seismic section on the left, and from a randomly chosen seismic trace (Trace no. 238) on the right. This comparison shows that the frequency content of each trace is almost identical to the rest of the seismic section, and we find the modes predicted by the previous spectrum. In the second part, we produced a histogram of the

seismic section Figure 3. The amplitude distribution follows a normal distribution centred around amplitude 0, which is also consistent. The seismic data are therefore of good quality for inversion. We will now proceed to QC the data through the Horizons.

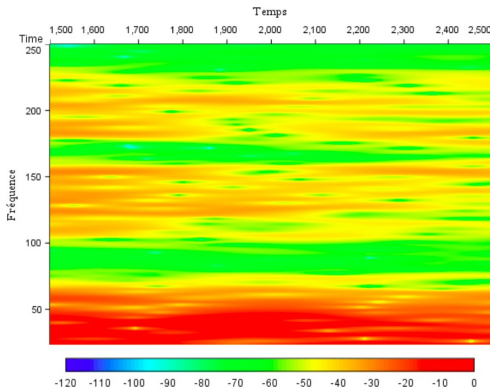


FIGURE 4 - Spectrogram corresponding to the seismic section at inline 100, whole seismic cube

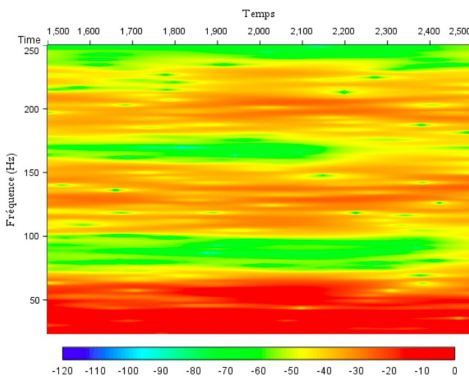


FIGURE 5 - Spectrogram corresponding to the seismic section at inline 100, for trace 238

2.2 QC data across horizons

We then imported geological data: horizons. These are impedance contrasts corresponding to a change in elastic property that can be linked to a geological age. These horizons are key markers that will later enable us to constrain and exhibit a subsurface model. It is essential to check the quality of the horizon data. For this study, we have three horizons named H1, H2 and H3. The H2 horizon is characterised as being the roof of the reservoir. Firstly, all our horizons need to be processed to make them *regular* objects in the Interwell sense. This involves gridding and smoothing the horizons. Gridding creates a more regular grid and fills in any gaps that may not have been marked. Smoothing makes the grid geometrically smoother. The modified and added points help to interpolate and smooth the horizon curve.

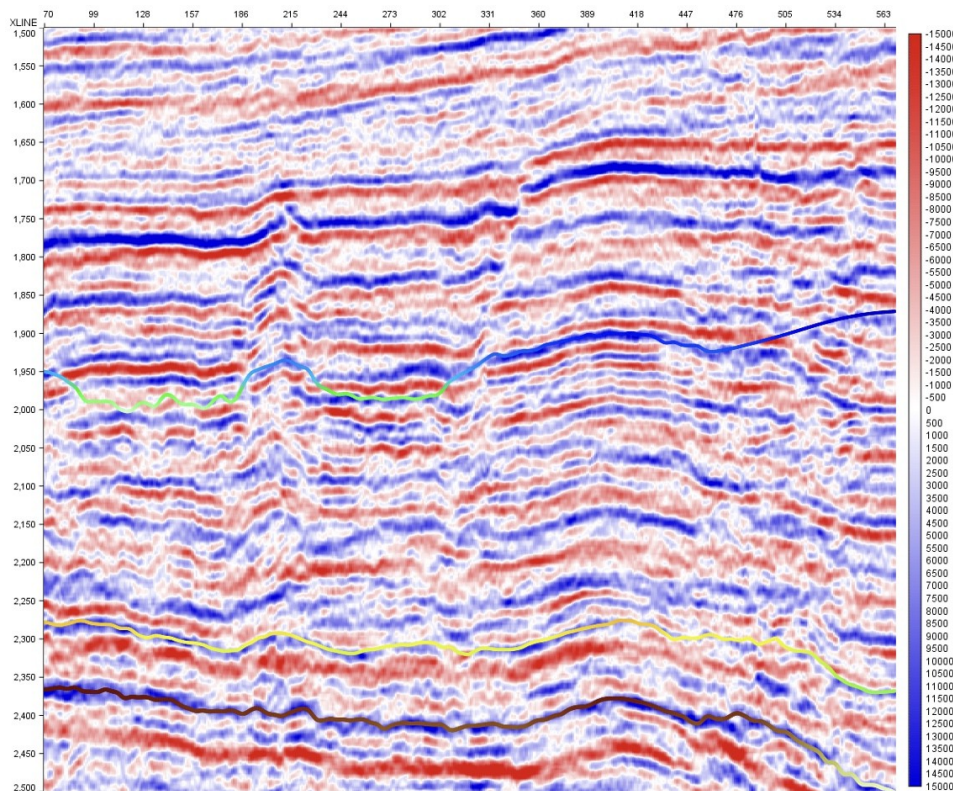


FIGURE 6 - Seismic section with horizons, from top to bottom H1 H2 H3

The dataset shown in Figure 6 contains the 3 horizons H1, H2 and H3. H2 corresponds to the top of the reservoir and H3 corresponds to the bottom of the reservoir. H1 is located at a shallower depth. In Figure 7, we can see the difference between the curve for the first horizon (light blue), and the curve after gridding (dotted blue) and smoothing (dark blue).

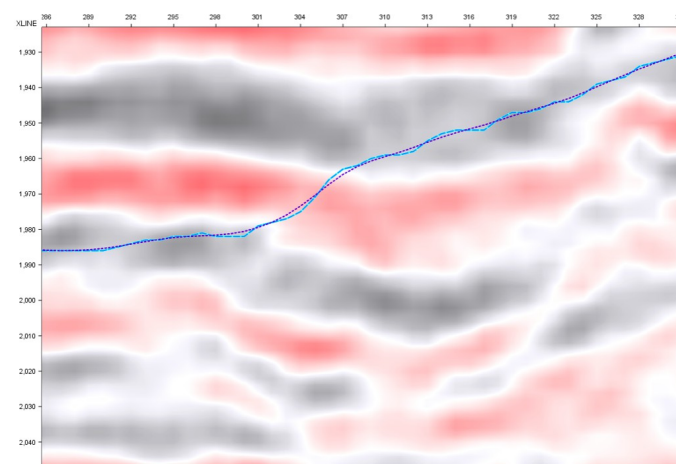


FIGURE 7 - Raw, gridded and smoothed H1 horizon superimposed on the seismic section

With these horizons we can calculate various maps: RMS amplitude map (Figure 9), amplitude correlation map (Figure 8).

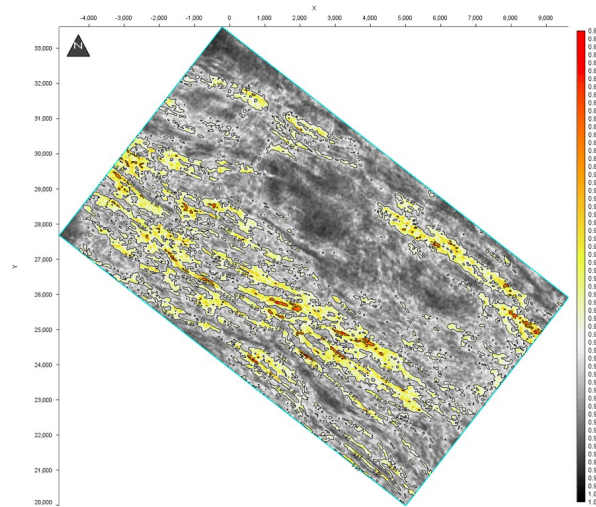


FIGURE 8 - Full Stack correlation map

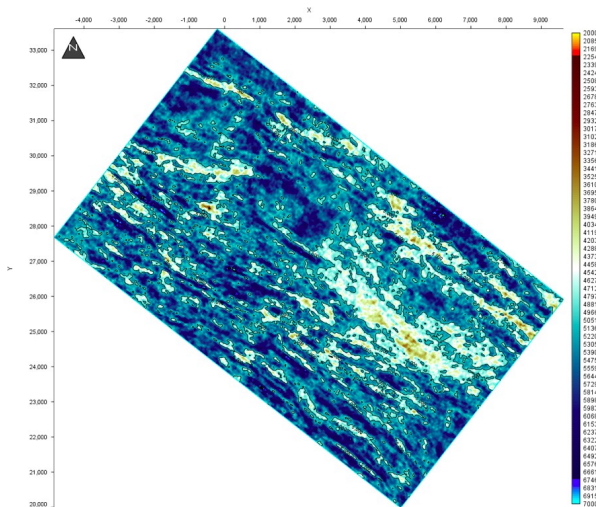


FIGURE 9 - Full Stack RMS card

These maps are not of major interest in the inversion process, but they do allow us to make an a priori interpretation, and at the same time ensure the quality of the horizon data.

2.3 QC well data

Finally, we import the well data for 6 wells: wells 1, 2, 3, 7, 24 and 28, the locations of which can be seen on the map (Figure 10, 11).

Note: All the wells are vertical, except for well 7 which is deviated, which we have not represented. The data associated with these wells are of various types: log data (P-wave travel time, S-wave travel time), bulk density, gamma ray, horizon markers, P-impedances given by $I_p = V_p * \rho$, S-impedances given by $I_s = V_s * \rho$ and elastic impedance.

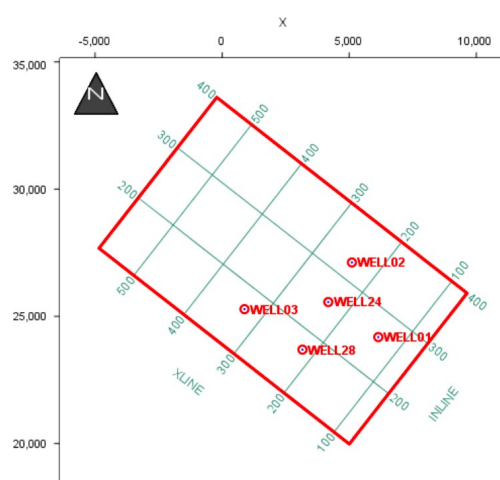


FIGURE 10 - Map of wells: location

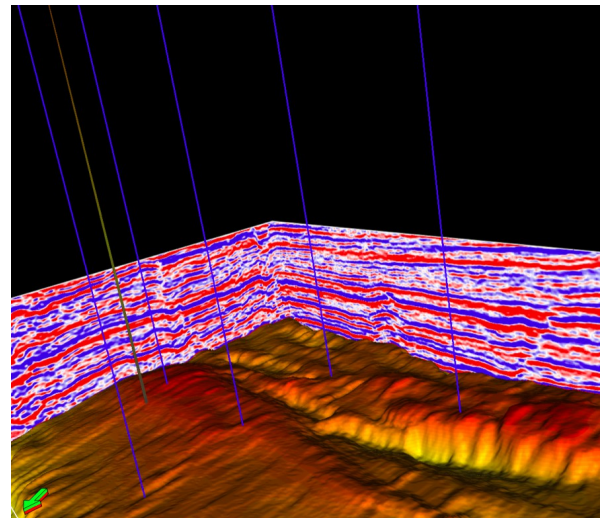


FIGURE 11 - Well in 3D view

Before using these well data, it is important to calibrate them with the seismic data recorded in TWT (Two-Way-Travel-time). We therefore imported the TWT law, which enables this conversion to be carried out. TWT can also be used to transform depth-dependent well logs into TWT logs, as shown in Figures 12 and 13. This processing allows us to transform acoustic impedance, elastic impedance and resistivity data. These data will be useful in the inversion process. Once the conversion has been carried out, the wells have been tuned with the seismic data, and the horizons have been processed in the previous section, it is possible to represent all our information.

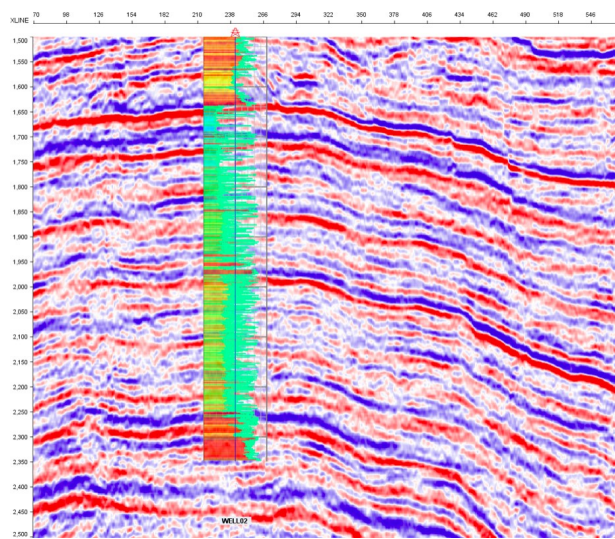


FIGURE 12 - Log of a well superimposed on seismic the

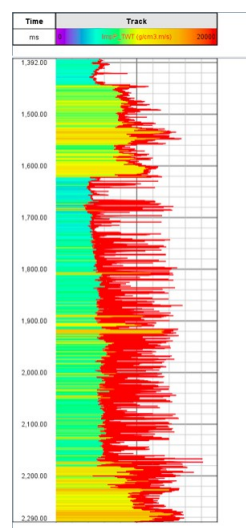


FIGURE 13 - Well log

3 Wavelet shape estimation

As a reminder, the inversion process is a deconvolution process. This involves deconvolving the seismic traces, in order to first obtain the reflectivity log, and then

impedance. The traces are deconvolved using a wavelet estimated statistically for the entire seismic survey. A key step is therefore the estimation of the wavelet, which must be carried out carefully. In our study we performed an elastic estimation, as Interwell allows acoustic inversion with an elastic wavelet.

3.1 Preliminary estimation of the elastic wavelet by MCA

The idea is to extract a wavelet from the seismic data alone. To do this, we will apply a Multi-Coherence Analysis (MCA) over a well-chosen time window. The MCA is a set of *cross-correlations* and *self-correlations* that enable a wavelet to be estimated from the seismic data alone. This wavelet is then truncated to reduce its length while retaining the high energy content of the signal. This reduces the calculation time for the convolutions, but also improves the convergence of the inversion. A low-pass filter is then applied to the selected portion of the wavelet to obtain a better signal-to-noise ratio. The choice of filter parameters (Figure 14) is very important, as poor filtering will not allow the missing frequencies to be imaged correctly.

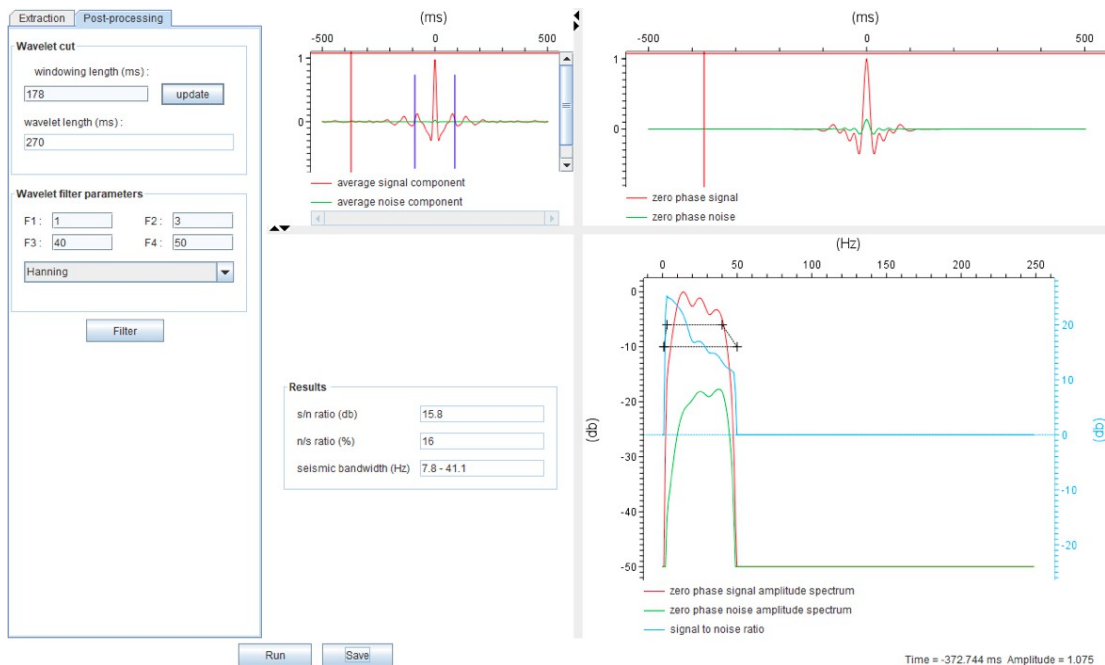


FIGURE 14 - Screenshot of wavelet extraction for full-stack

The MCA was applied to our different stacks (Full-Near-Mid-Far). Figures 15 and 16 show the results obtained for the different stacks.

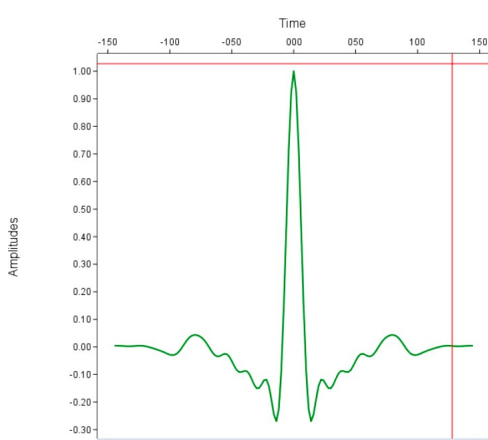


FIGURE 15 - FULL STACK MCA corrugator

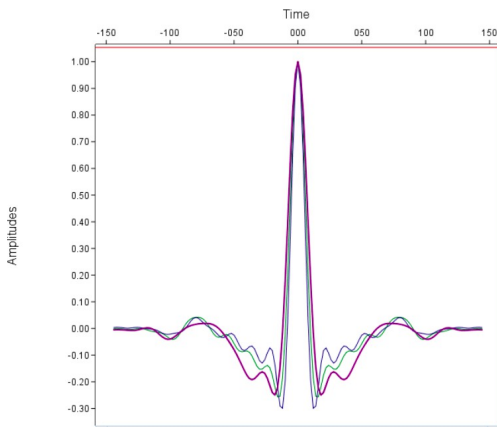


FIGURE 16 - Wavelets Near(blue)
Mid(green) Far(purple) superimposed after
MCA

3.2 Wavelet optimisation from well data

The second part of the elastic wavelet estimation includes the analysis of the well data. As the elastic impedance logs contained more high frequencies than the seismic, these logs had to be filtered in order to obtain signals with a frequency content similar to that of the seismic. The wavelet modelled by MCA will be used to create a synthetic trace for well calibration. To obtain the synthetic trace representing the well data, the MCA wavelet is convolved with the filtered impedance log. The synthetic trace is duplicated and positioned at the well location.

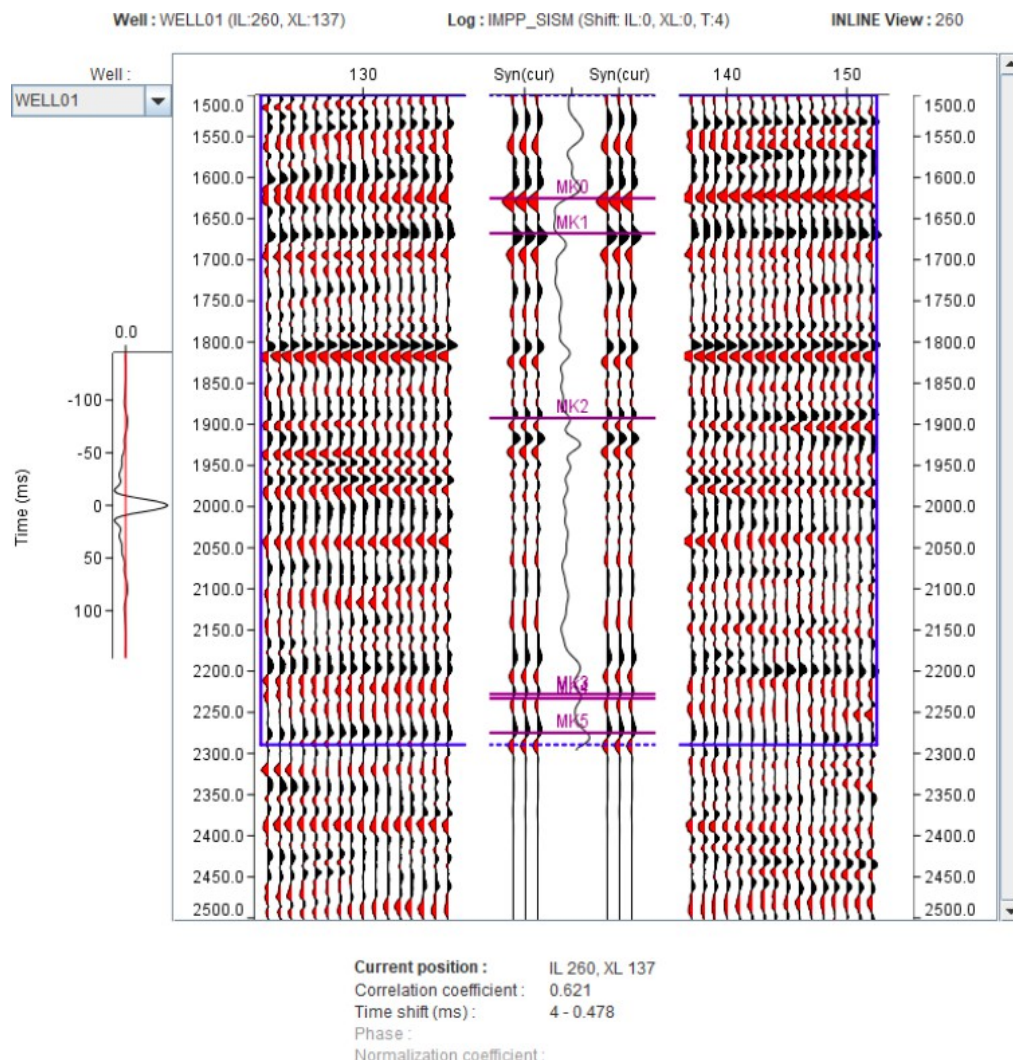


FIGURE 17 - Calibration of wells using Time-Shift

The aim is to match the wavelets as closely as possible to the wells and angle-stacks (Full-stack in our case), in order to obtain the best possible statistical wavelet. This wavelet is extracted in three successive stages:

- Time-shift estimation: This step consists of shifting the synthetic traces representing the wells along the time axis, in order to maximise the correlation between the synthetic traces and neighbouring traces.
- Determining the phase rotation: This step consists of changing the phase of the wavelet in order to maximise the correlation between the synthetic traces calculated in the well and the neighbouring traces.
- Energy normalisation coefficient: This involves finding the amplitude of the wavelet that maximises the correlation. It is important to normalise the amplitude of the wavelet correctly, because a wrong amplitude value will affect the value of the reflection coefficient. These wavelet optimisation steps are carried out taking into account all the wells (except 7). This is a statistical approach. This strategy also makes it possible to virtually change the location of the well in order to find the position that maximises the correlation, see Figure 18.

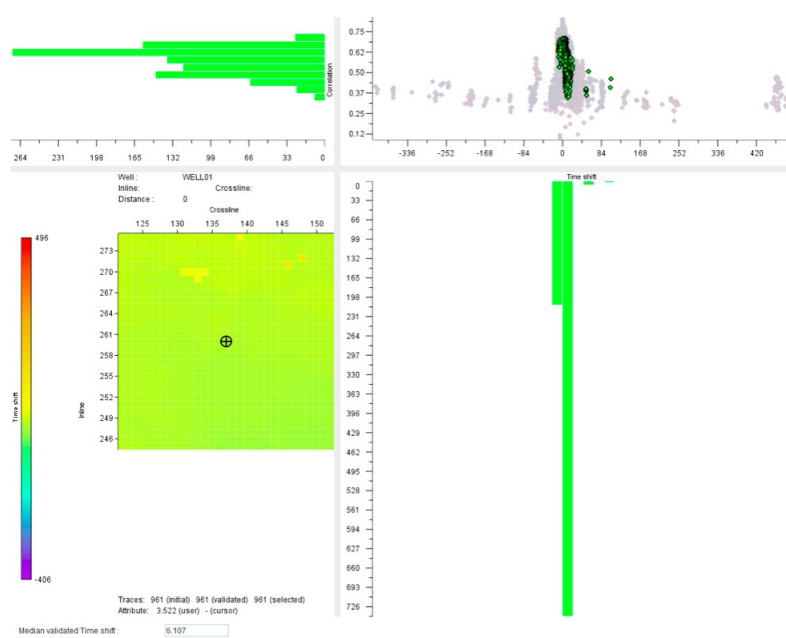


FIGURE 18 - Data selection for wavelet estimation

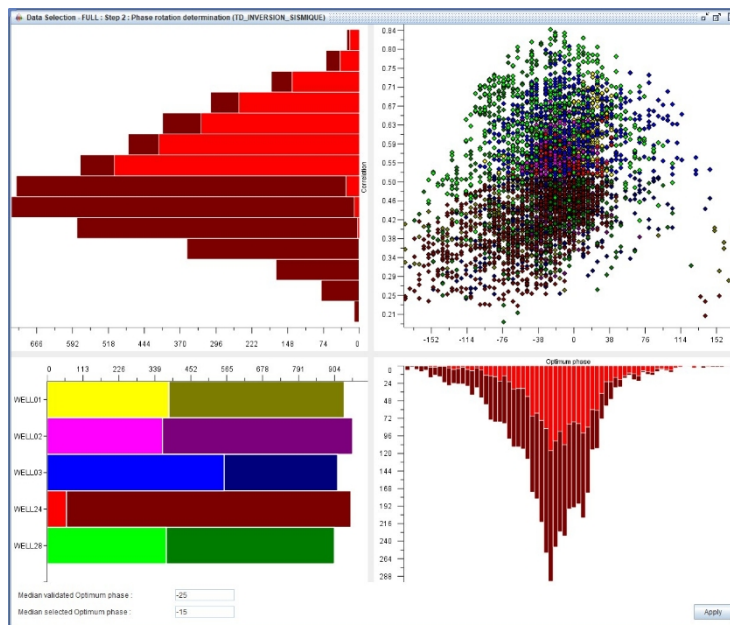


FIGURE 19 - Data selection for wavelet phase estimation

In Figure 19, the wells are colour-coded and the correlation values are plotted against the optimum phase. Bright red corresponds to the values selected automatically and dark red are the data that are rejected. The operator can change this selection.

Another way of selecting the data is to display it as a map around the wells, as shown in Figure 18. This figure shows the actual location of the well on the map, in the form of a circle, the location with the maximum correlation in the form of an oblique cross, and the operator can choose the location to be applied to the well by

placing the cross. The location with the maximum correlation is chosen by default, and once again can be modified by the operator.

The final step is to evaluate the normalisation coefficient that will be applied to the wavelet, as shown in Figure 20.

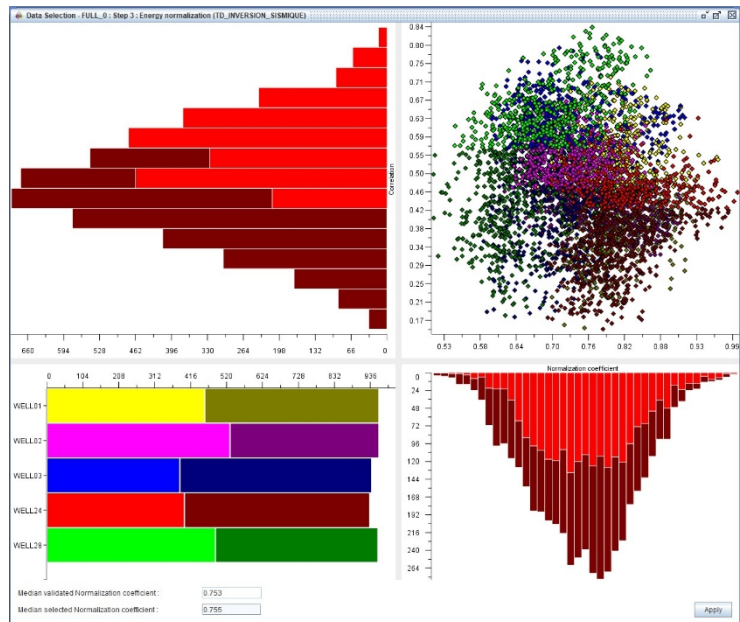


FIGURE 20 - Data selection for wavelet energy estimation

3.3 Final wavelet

Here we summarise in a table the various values obtained during our wavelet analysis and extraction. In Figure 21 below, we show the final Full- Zero Mean wavelet in green (superimposed on those of the wells).

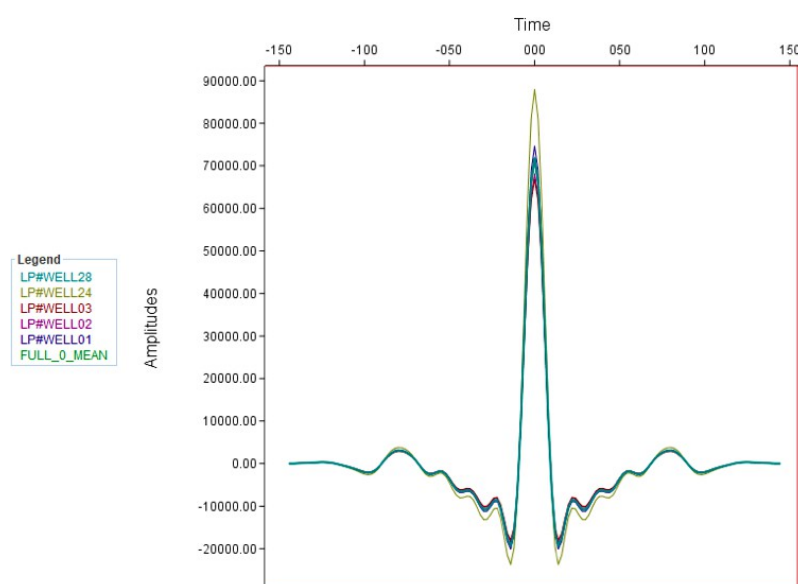


FIGURE 21 - Final wavelet with phase rotation and energy

Coefficient of correlation	Time-Shift (ms)	Phase (°)	Coefficient of standardisation
0.724	4 - 0.05	0	0.795
0.724	4 + 0.468	10	0

4 Reverse

4.1 Building the initial model

In this section we have created an a priori impedance model. The inversion carried out by Interwell is based on an initial model which will then be updated in order to best explain the observed data. We have created a framework that presents a simple structural geology model with horizons: Figure 22. The geological units of deposition and their geological ages can be seen in Figure 23.

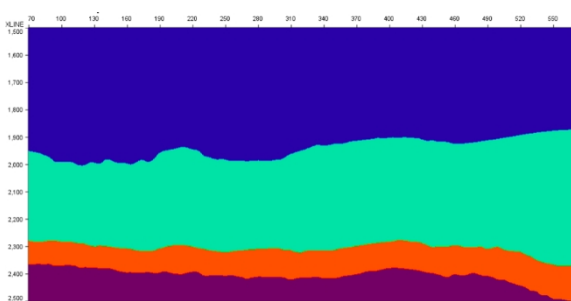


FIGURE 22 - Struct.MLID a priori model

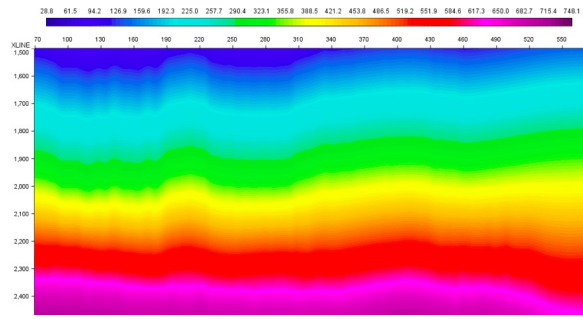


FIGURE 23 - Smoothed and interpreted horizons (struct.AGE)

4.2 Model-based inversion

Acoustic inversion is used to model the impedance P (IP). Figure 24 shows the variation in dips, which also coincide with the horizons. The blue colours indicate downward dips and the red colours upward dips. The horizons and dips are the basic stratigraphic data needed to fill the frame with the inversion. The proposed stratigraphy is not complicated, because we want our initial model to provide the very low frequencies that are absent from the seismic, without being too complex. The initial model should not constrain the inversion too much, unless we have a high degree of confidence in our geological data. Figures 23 and 25 show the a priori model based on the geological and dip analyses, but also on the impedance logs from the calibrated well data. This is the model that Interwell will use for the inversion.

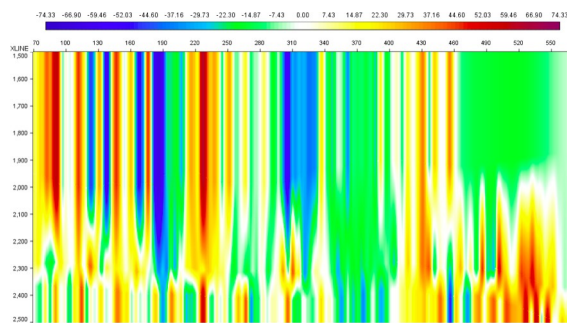


FIGURE 24 - Pendants (struct.DIPX)

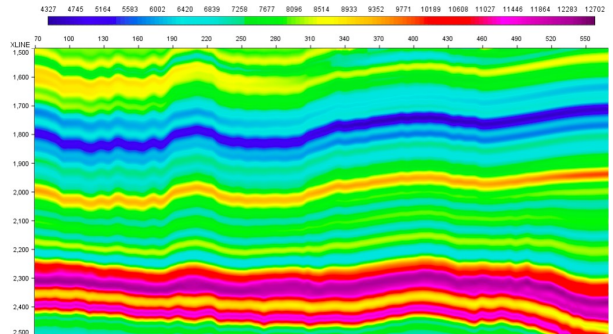


FIGURE 25 - A priori impedance model

Interwell inversion is achieved by minimising an objective function. The special feature of this objective function is that it contains a term for seismic and a term for geology. This makes it possible to assign a degree of confidence to the seismic or geological knowledge we have of our environment. So you can choose to follow the geology as closely as possible, even if it means having a higher error rate for seismic, or vice versa.

5 Inversion results

5.1 Synthetic seismic

The inversion performed by Interwell provides several results, including the IP acoustic inversion result in Figure 26 and the synthetic seismic result in Figure 27. The synthetic result is obtained by convolution of the acoustic impedance response and the wavelet.

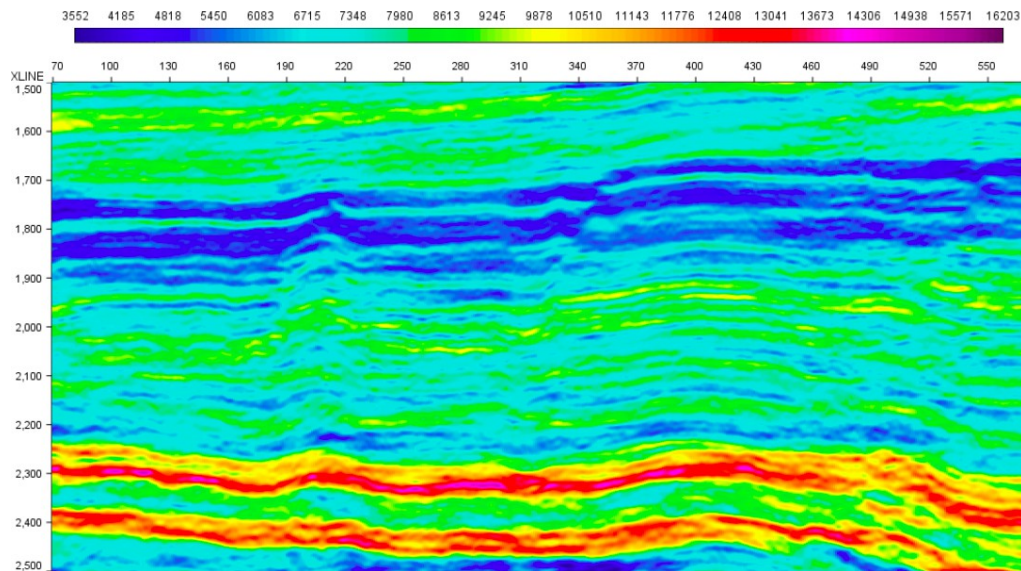


FIGURE 26 - Acoustic inversion result P wave impedances

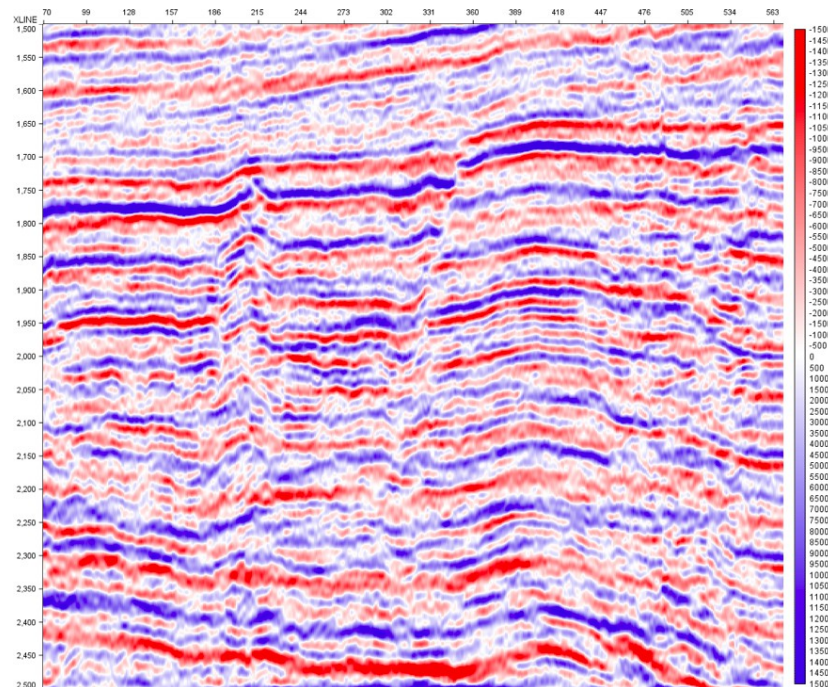


FIGURE 27 - Synthetic seismic data obtained using the software

5.2 Comparison of synthetic and real seismic data

The synthetic seismic figure (Figure 27) shows the gain in low frequency brought about by inversion. A simple way of quantifying this result is to look at the residual in Figure 28 between the real seismic and the synthetic seismic. This result can be explained by the fact that, thanks to the well data included in the inversion, it is possible to incorporate low frequencies into our synthetic seismic.

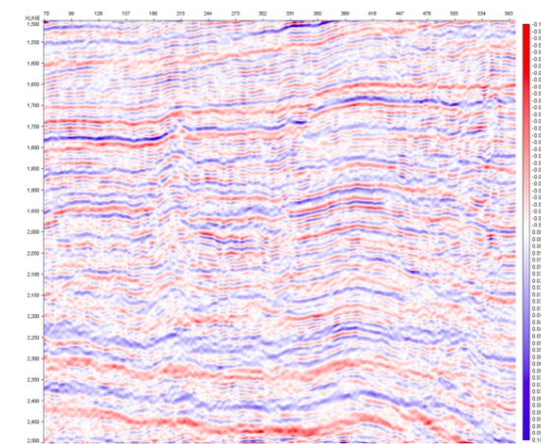


FIGURE 28 - Difference between our seismic data and the synthetic seismic data obtained by the software

5.3 QC on inversion by comparison with real data

Figure 28 shows the differences between our seismic and the synthetic seismic obtained by the software. We can see that the values are very close to zero (see scale

colorbar ± 0.100), so this confirms that the inversion is close to the reality of our seismic.

Furthermore, the synthetic wavelet is almost identical to the extracted wavelet, except for the lobes furthest from the symmetry axis (Figure 29).

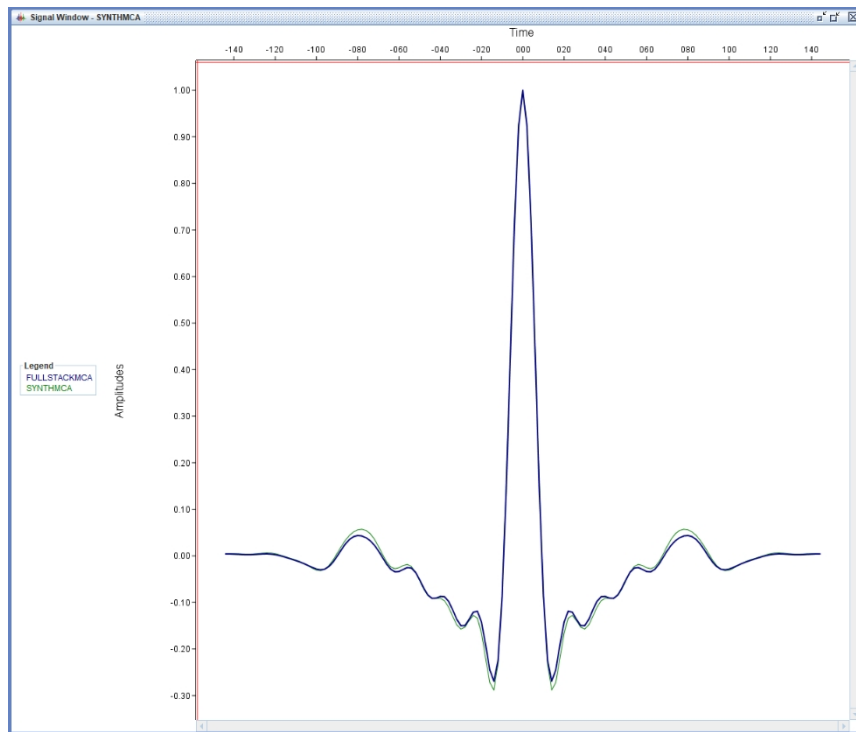


FIGURE 29 - Synthetic wavelet after inversion

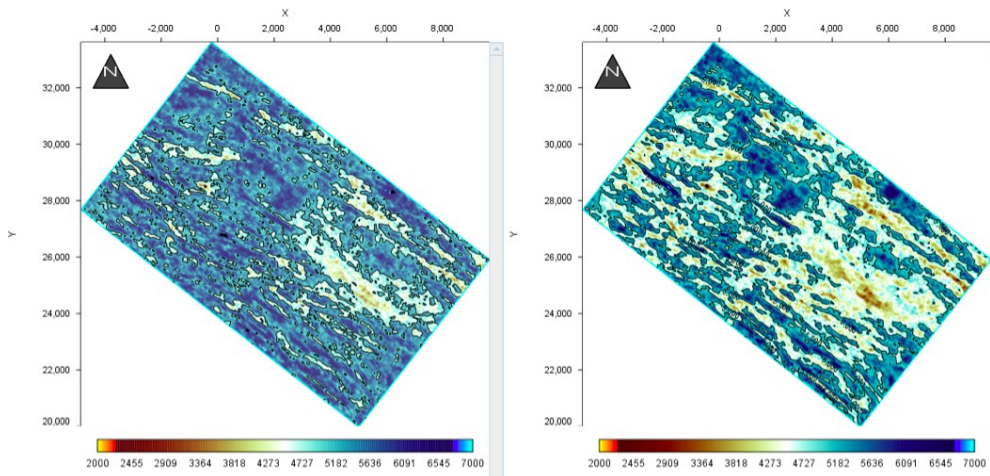


FIGURE 30 - Comparison of seismic RMS on the left and synthetic RMS on the right

6 Conclusion

The Interwell software enabled us to visualise the data and use it to perform elastic and acoustic inversions, and to deduce the physical properties of the subsoil. These inversions reveal the presence of geological layers

and, in particular, the presence of a reservoir at depth. This tool is very useful and easy to use, and can be used to perform many QCs and calculations.